RSC Advances

ROYAL SOCIETY OF CHEMISTRY

www.rsc.org/advances

Highly efficient loading of doxorubicin in Prussian Blue nanocages for combined photothermal/chemotherapy against hepatocellular carcinoma

Ming Wu [a,b,#], *Qingtang Wang* [a,b,#], *Xiaolong Liu* *[,a,b], *Jingfeng Liu* *[a,b,c]

[a] The United Innovation of Mengchao Hepatobiliary Technology Key Laboratory of Fujian Province, Mengchao Hepatobiliary Hospital of Fujian Medical University, Fuzhou 350025, P. R. China

[b] The Liver Center of Fujian Province, Fujian Medical University, Fuzhou 350025, P. R. China

[c] Liver Disease Center, The First Affiliated Hospital of Fujian Medical University, Fuzhou 350005, P. R. China

ABSTRACT: Prussian Blue-based nanoparticles have been explored as the new generation of NIR-driven photothermal conversion agent (PTCA) for cancer treatment. However, PTT treatment alone has limited therapeutic efficiency since it could not eliminate tumor cells completely. In this paper, we synthesized Prussian Blue nanocages (PBNCs) loaded with doxorubicin (DOX) (referred to as PBNCs-DOX nanocomposites) as efficient drug delivery vehicles, combining with photothermal therapy function of Prussian Blue and chemotherapy function of DOX to enhance the therapeutic efficiency against hepatocellular carcinoma (HCC). The prepared PBNCs-DOX nanocomposites were characterized by TEM and the FT-IR spectra. Fluorescence intensity (FI) measurements determined that the loading content of DOX in PBNCs was as high as 33.0 wt% and that the loading efficiency was even up to 88.4 %. The DOX release from the PBNCs could be triggered by the environmental pH and near infra-red (NIR) laser irradiation. In vitro cytotoxicity assay demonstrated that the PBNCs-DOX nanocomposites had significantly higher killing efficacy against HepG2 cells in the presence of NIR irradiation, than those in the absence of NIR irradiation or those in the presence of NIR irradiation but treated with PBNCs rather than PBNCs-DOX nanocomposites. Therefore, PBNCs-DOX nanocomposites, which have integrated the photothermal therapy together with the chemotherapy, might serve as promising dual-mode therapeutic agents for HCC treatment in the future.

KEW WORDS: Prussian Blue nanocages (PBNCs); Doxorubicin (DOX); Photothermal therapy; Chemotherapy; pH and photothermal triggered drug release

1 Introduction

Hepatocellular carcinoma (HCC) is one of the most lethal malignant cancers worldwide, which were mostly diagnosed at late and advanced stages[1]. Up to now, the therapeutic efficiency of the primary curative treatments for HCC including surgical resection, chemotherapy, radiotherapy, ablative therapy and transarterial chemoembolization, are still unsatisfactory[2], due to their high frequency of tumor recurrence and strong systemic toxicity[3]. Therefore, it is an urgent need to develop new systematic therapeutic approaches for HCC treatments.

Photothermal therapy (PTT) is a non-invasive laser-based therapy technology, which employs photothermal conversion agent (PTCA) to "heat" cancer tissue and cells under laser irradiation[4], and has been increasingly recognized as a promising alternative method comparing to the conventional approaches for cancer treatment. Due to the minimal absorption of near-infrared (NIR, λ = 700–1100 nm) light and the optimal penetration depth in biological tissue, ideal PTCA should exhibit strong absorption in the NIR region and high photothermal conversion efficiency[5, 6]. However, complete eradiation of tumor cells with PTT alone is difficult because of heterogeneous laser heat distribution and limited light penetration[7, 8]. In order to obtain sufficient heating in cancer cell killing and tissue ablation, the relative high laser power is needed in clinical cancer treatment, which maybe hurts normal tissues. Multi-mode therapeutic nanoplatform which is combining PTT with other therapeutic

technologies (such as chemotherapy) has the potential to effectively reduce the laser power of PTT, which could avoid the damage of healthy tissues, and enhance the cure rate of cancer treatment due to the synergistic effect[9-12]. In recent years, various systems which are able to co-delivery of chemotherapeutic agents together with PTCAs to the tumor regions, have been developed[8, 13, 14]. In these systems, Au-based nanoparticles functionalized with DOX were most extensively studied as the PTT/chemotherapy agents[10-12, 15-18]. However, these nanomaterials have either low drug loading capacity, or are concerned with the biological safeties in long term in vivo.

Prussian Blue (PB) is a clinic drug approved by the USA Food and Drug Administration (FDA) for the treatment of radioactive exposure[19], and PB nanoparticles have also been developed as a new generation of PTCA due to their high absorption in NIR region[5, 20-23]. However, the PB nanoparticles without hollow or porous structures cannot encapsulate drugs with a high efficacy. Recently, Yamauchi group[24, 25] have fabricated a novel Prussian Blue nanocages (PBNCs) with hollow interior cavity and porous outer shell, and it has been applied to loaded cisplatin and the loading efficacy was almost achieving 100%, but only 5% of the loaded drugs could be released even after 200 min incubation. Furthermore, the PTT function of the PBNCs and their combination effect with cisplatin have not been investigated in their report[25].

Inspired from the high payload of drug into the hollow and porous nanoparticles[12, 14], in this work, we fabricated PBNCs as the hydrophobic drug delivery vehicles for DOX and further studied their combination effects of PTT/chemotherapy against HepG2 cells. To the best of our knowledge, the combination therapy effect of Prussian Blue nanoparticles (PTT) and DOX (chemotherapy) have not been reported previously. Here, the prepared PBNCs-DOX nanocomposites were characterized by TEM and the FT-IR spectra; the highly payload ability of DOX in PBNCs, the photothermal conversion efficiency and the pH sensitive drug release behavior were also carefully investigated. Furthermore, the combinated therapeutic effect of PTT/chemotherapy of the PBNCs-DOX nanocomposites was studied by using CCK-8 assay and Calcein AM staining.

2 Experimental

2.1 Materials

Polyvinylpyrrolidone (PVP, average *M*w=40000) were purchased from Sigma-Aldrich. Doxorubicin hydrochloride (DOX•HCl) was purchased from Hefei Biomei biotechnology. Cell Counting Kit-8 (CCK-8) was obtained from Dojindo Laboratories. $K_3[Fe(CN)_6]$ (AR), hydrochloric acid (AR), dimethyl sulfoxide (DMSO,AR), sodium hydroxide (NaOH, AR) were purchased from Sino pharm Chemical Reagent and used without further purification. Hoechst 33342 and DAPI were purchased from Sigma-Aldrich, Calcein AM and Lysotracker Green DND-26

were purchased from Life Technologies. Deionized (DI) water (18.2 MΩ·cm, 25℃) was obtained from Milli-Q Gradient System (Millipore, Bedford, MA, USA) and used in all experiments.

2.2 Instruments

FT-IR spectra of the samples (including PBNCs, standard of the DOX and PBNCs-DOX nanocomposites) were collected on an FT-IR spectrometer (Nicolet, USA). The morphology and particle size of the samples were characterized by TEM (Tecnai F20, FEI, USA) operated at 200 kV. Dynamic light scattering (DLS) experiments were performed at 25℃ on a NanoZS (Malvern Instruments, UK) with a detection angle of 173°, and a 3 mW He-Ne laser operating at a wavelength of 633 nm. The Z-average diameter and the polydispersity index (PDI) values were obtained from analysis of the correlation functions using cumulants analysis. The Vis-NIR absorption spectra and the fluorescence intensity (FI) of DOX, PBNCs and PBNCs-DOX nanocomposites were detected by a Spectra Max M5 microplate reader (Molecular Devices, USA) at excitation wavelength of 474 nm and emission wavelength of 590 nm. Near infrared reflection (NIR) laser irradiation was conducted with a continuous-wave diode NIR laser at the central wavelength of 808 nm and the power density of 2 W/cm^2 (Beijing Kaipulin Optoelectronic, China). The temperature of the solutions was recorded with a thermocouple microprobe STPC-510P (Xiamen Baidewo, China). Confocal fluorescence microscopy studies were performed with a

Nikon A1R-AI Confocal Microscope System with 488-nm laser excitation for calcein AM, 405-nm for DAPI and 543-nm for DOX.

2.3 Cell culture

HepG2 cells, a human HCC cancer cell line, were maintained as monolayer culture in RPMI-1640 medium supplemented with 10% fetal bovine serum (Atlanta Biologicals, USA) and 1% penicillin-streptomycin (Gibco BRL, USA) at 37°C in a humidified atmosphere (5% CO_2), while the noncancerous NIH/3T3 cells were cultured in DMEM medium at the same conditions .

2.4 Preparation of the DOX-loaded PBNCs

PBNCs were prepared according to the reported literature with a few modifications[24]. Briefly, PVP (6 g) and $K_3[Fe(CN)_6]$ (113.1 mg) were added into round-bottom flask containing 40 mL HCl solution (0.01M) with magnetic stirring. Untill a clear solution was obtained, the flask was heated to 80°C and maintained at this temperature for 20 h. Then, the resulted free nanoparticles in the solution were collected by centrifuging at 40000 g for 20 min, and washed with 40 mL of DI water for three times. After drying in vacuum at 50°C for 12 h, the Prussian Blue nanoparticles were obtained. For the preparation of PBNCs, the Prussian Blue nanoparticles (20 mg) and PVP (100 mg) were added to a Teflon vessel containing 20 mL HCl solution (1.0 M). After magnetic stirring for 2 h, the vessel was transferred into a stainless autoclave and heated at 140°C for 4 h in an electric oven. After that,

the autoclave was cooled down to room temperature naturally. The obtained nanoparticles were collected by centrifuging at 50000 g for 10 min, and washed with 20 mL of DI water for three times. After drying in vacuum at 50°C for 12 h, the PBNCs were obtained.

DOX was incorporated into PBNCs using nanoprecipitation method. Briefly, PBNCs were dispersed into DI water, and the final concentration of PBNCs solution was adjusted to 0.5 mg/mL. DOX•HCl (final concentration: 0.25 mg/mL) was subsequently added into above PBNCs solution under ultrasonication. Then the mixtures were transferred into a sealed vial and then 1 M NaOH solution was added drop wise under magnetic stirring to neutralize the HCl. After that, the mixture was stirred at 1000 rpm at room temperature for 24 h under dark conditions to allow the penetration of DOX through the porous channels and deposition into the hollow interiors of PBNCs. Precipitates were collected by centrifuging above mentioned reaction solution, and washed with equal volume of DI water for three times. After drying in vacuum at 50°C for 12 h, the PBNCs-DOX nanocomposites were obtained.

The amount of DOX loaded in PBNCs was analyzed as follows. 0.28 mg of nanocomposites were dispersed in 1 mL DMSO, and sonicated for 5 min to ensure complete dissolution of the DOX from PBNCs. The supernatant was then collected for FI measurement after complete centrifugation of the dispersion. The fluorescence intensity of the supernatant was determined using a SpectraMax M5 microplate reader

at the excitation wavelength of 474 nm and emission wavelength of 590 nm, and the concentrations of DOX were obtained from a calibration curve, which was linear over the concentration of DOX from 0.1μg/mL to 4μg/mL with a correlation coefficient of R^2=0.995.

Encapsulation efficiency= (weight of DOX loaded into the PBNCs)/(initial feeding weight of DOX).

Loading content = (weight of DOX loaded into the PBNCs)/(weight of the PBNCs + DOX loaded into the PBNCs)

2.6 In vitro drug release

In order to evaluate the drug release behavior of DOX loading in PBNCs, PBNCs-DOX nanocomposites (DOX concentration 26.74 μg/mL) were dispersed in 1 mL of buffer solutions with ultrasonication at pH values of 7.2 (phosphate buffer solution, 10 mM), 6.5 (phosphate buffer solution, 10 mM) and 4.8 (acetate buffer, 10 mM) respectively, and then stirred at 37 °C. At determined time intervals, above solutions were centrifuged at 50000 g for 10 min at 4 °C, and 500 μL of supernatants were withdrawn while the same volume of counterpart fresh buffers were added to the residual composite solutions. The amount of released DOX in the supernatant was determined by detecting the fluorescence intensity of DOX. To study whether the DOX release from the nanocomposites could be triggered by the NIR laser irradiation, the nanocomposites solutions were irradiated with the NIR laser (808 nm, 2 W/cm^2)

for 5 min at the predetermined time intervals, followed by centrifugation and the supernatants were collected for analysis of the released DOX. All experiments were performed in triplicate. Results were presented as mean ± standard deviation (SD).

2.7 In vitro cytotoxicity assay

A CCK-8 assay was carried out to investigate the cytotoxicity of PBNCs without DOX loaded and PBNCs-DOX nanocomposites. In a typical experiment, NIH/3T3 cells were first seeded in a 96-well plate with density of 1×10^4 cells per well at 37℃ in a humidified atmosphere (5% CO_2) for 24 h. Then, the cell culture medium was discarded, and the cells were washed three times with PBS to remove dead cells. After that, the cells were incubated with gradient concentrations of nanoparticles (PBNCs concentration: 0, 1.56, 3.12, 6.25, 12.5, 25, 50, 100μg/mL) dispersed in fresh medium for 24 h, respectively. Then after the cells were washed three times with PBS to remove free composites, the CCK-8 assay was used to detect the cell survival rate according to the manufacturer's protocol. Cell viability was calculated as follows: cell viability (%) = $(OD_{sample}-OD_{blank})/(OD_{control}- OD_{blank}) \times 100$. The OD_{sample} and $OD_{control}$ are the absorbance values of the treated cells (as indicated) and the untreated control cells (without composites), respectively. The OD_{blank} was the absorbance of CCK-8 itself at 450 nm measured by the SpectraMax M5 microplate reader. All experiments were performed in quadruplicate. Results were presented as mean ± standard deviation (SD).

2.8 Evaluation of the photothermal performance

The evaluation of photothermal performance of PBNCs and PBNCs-DOX nanocomposites was carried out by monitoring the temperature of 1.0 mL nanoparticle solution at gradient concentrations (PBNCs concentration: 0, 12.5, 25, 50, 100 μg/mL) induced by NIR laser irradiation. Briefly, 1 mL of nanoparticle solution was added to a quartz cuvette and irradiated by NIR laser with the wavelength of 808 nm at the power density of 2 W/cm^2 for 5 min. The temperature of the sample solution was measured by using a digital thermometer (with an accuracy of 0.1 °C) with a thermocouple probe. Meanwhile, 1mL DI water was used as a control.

2.9 Cancer cell ablation efficiency of PBNCs-DOX nanocomposites

Cancer cell ablation efficiency of PBNCs-DOX nanocomposites on HepG2 cells was qualitative evaluated using confocal microscopy. Typically, HepG2 cells (5×10^4) were seeded onto 35 mm glass-bottom Petri dish and cultured for 24 h at 37 °C in the incubator. Then the culture medium of above cells was replaced with nanocomposites dispersion in fresh culture medium and the cells were incubated for another 24 h in the incubator. Subsequently, fresh culture medium was added and the cells were exposed to NIR laser radiation (2 W/cm^2) for 2 min, after that the cells were washed three times with PBS to remove free nanocomposites. Finally, the cells were washed with PBS and stained with 2 μM calcein AM for the visualization of living cells with confocal fluorescence microscope with 488-nm laser excitation.

To further investigate the cancer cell ablation efficiency of PBNCs-DOX nanocomposites quantitatively, the CCK-8 assay was used. HepG2 cells with density of 1×10^4 cells per well were first seeded in a 96-well plate at 37°C in a 5% CO_2 atmosphere for 24 hours. Then, the cell culture medium was discarded, and the cells were washed three times with PBS to remove dead cells. After that, the cells were incubated with PBNCs, DOX (equivalent concentration to the DOX in the nanocomposites), and our nanocomposites for 24 h, respectively. Afterwards, the cells were exposed to NIR laser (808nm, 2W/cm^2) for 2 min as indicated. Then after the cells were washed three times with PBS to remove free nanocomposites, the CCK-8 assay was used to detect the cell survival rate according to the manufacturer's protocol. All experiments were performed in quadruplicate. Results were presented as mean ± standard deviation (SD).

2.10 Confocal microscopy study of cellular uptake of PBNCs-DOX

Cell uptake of PBNCs-DOX nanocomposites was performed on HepG2 cells using confocal microscopy. HepG2 cells (3×10^4) were seeded onto 35 mm glass-bottom Petri dish and cultured for 24 h at 37 °C in the incubator. Then the culture medium of above cells was replaced with PBNCs-DOX nanocomposites (DOX: 10 μg/mL) dispersion in fresh culture medium and the cells were incubated for another 4 h in the incubator, while the cells of control group were incubated with only fresh culture medium. After that, the cells were washed three times with PBS to

remove free nanocomposites. Finally, the cells were fixed with 4% paraformaldehyde in PBS for 15 min, and the nuclei were then stained with 5.0 μM DAPI. Cells were imaged by confocal microscopy (Nikon A1R-AI Confocal Microscope System) with 543 nm laser excitation for DOX and 405 nm laser excitation for DAPI.

To investigate more details of the cellular uptake of the nanoparticles and the pH sensitive drug release behaviour, HepG2 cells were incubated with PBNCs-DOX nanocomposites dispersion (DOX: 10 μg/mL) for 1 h, 4 h and 24 h, and free DOX-treated cells were used as control. After incubation, the drug-containing solutions were removed and 1 μM Lysotracker Green DND-26 (an acidic organelle dye, Ex 504 nm, Em 511 nm) was added. After 20 min incubation, 5 mg/ml Hoechst 33342 (a nuclear dye, Ex 345 nm, Em 478 nm) was further added and incubated for another 10 min. Afterwards, the cells were carefully washed by pre-warmed culture medium for 3 times, then subjected to confocal laser scanning microscopy analysis.

2.11 NIR laser-triggered drug release behaviour of PBNCs-DOX nanocomposites in HepG2 cells

To evaluate the NIR laser-triggered drug release behaviour of PBNCs-DOX nanocomposites, HepG2 cells were incubated with PBNCs-DOX nanocomposites dispersion (DOX: 3 μg/mL) for 4 h, and free DOX-treated cells were used as a control. After incubation, the drug-containing solutions were removed and the cells were left un-irradiated or exposed to NIR laser irradiation (808 nm, 2 W) for 2 min,

respectively. Finally, the cells were fixed with 4% paraformaldehyde in PBS for 15 min, and the nuclei were then stained with 5.0 μM DAPI for 10 min. Cells were imaged by confocal microscope (Zeiss LSM780) with 543 nm laser excitation for DOX and 405 nm laser excitation for DAPI.

3 Results and discussion

3.1 Preparation and characterization of PBNCs-DOX nanocomposites

The overall experimental design and synthetic strategy are schematically illustrated in Fig. 1. The as-prepared PBNCs were obtained by using a "surface-protected etching" approach[26]. During the process of preparation, PVP firstly absorbed onto the surface of Prussian Blue nanoparticles to form a protection layer due to the binding of its amide group to iron ions[27], and then the PVP protection layer would decrease the etching rate on particle surface while the etching rate to interior of Prussian Blue nanoparticles was not affected[24, 26]. So the nanoparticles with hollow interior cavity and porous shell were formed and named as PBNCs. The PBNCs with the above structures were endowed with the potential as drug delivery vehicles. Hence in this work, DOX was loaded into PBNCs using a nanoprecipitation method[28]. The DOX molecules would penetrate through the porous shell and precipitate into the hollow interior cavity of PBNCs.

In order to further study this nanoprecipitation process, the dependence of DOX concentration on the morphology of the obtained drug-loaded nanoparticles was

further investigated by TEM and DLS experiments. As shown in TEM (Fig. 2A), the average size of PBNCs without drug loading was about 80 nm. The transparency of the cores of the PBNCs confirmed their cube-shaped hollow characteristics. The shell with a thickness of around 15 nm exhibited an obvious porous structure. DLS experiment (Fig. 3A) revealed that the average hydrodynamic size of PBNCs was 209.6 nm, and the PDI value of 0.281, which showed good disperse distribution of PBNCs. The average hydrodynamic size of PBNCs is larger than their size determined by TEM, which might be attributed to slight aggregation of a few nanoparticles obtained from water phase synthesis[29]. When the initial feeding DOX•HCl content was 0.25 mg/mL, nearly all the DOX molecules deposited in PBNCs as there was no apparent increase for the average size of the nanocomposites compared with initial PBNCs (Fig. 2A and Fig. 2B), and DLS experiment revealed the hydrodynamic size was not obviously changed. However, as the feeding amount of DOX•HCl was further increased to 0.5 mg/mL, large DOX aggregations could be observed in addition to the PBNCs (Fig. 2C), and even more serious aggregation was observed at same feeding conditions while without the usage of PBNCs (Fig. 2D). Additionally, DLS experiment (Fig. 3A) revealed the remarkable increase of average hydrodynamic size of nanocomposites (reached to 601.8 nm) and relatively weak disperse distribution (PDI value of 0.411). These results demonstrate that DOX molecules are preferentially deposited into the interior hollow cavity of PBNCs and the PBNCs are functional as precipitation templates in the loading process. The initial

feeding concentration of 0.25 mg/mL of DOX was used for further studies.

The successful loading of DOX into PBNCs was further confirmed using FT-IR spectroscopy which could identify the chemical groups of DOX, PBNCs and PBNCs-DOX nanocomposites (Fig. 3B). The peaks at 2086 cm^{-1} (attributed to the CN stretching in the Fe^{2+}-CN-Fe^{3+}) and 1656 cm^{-1} along with a shoulder peak around 1600 cm^{-1} (attributed to the C=O stretching vibration of PVP amide unit), were the typical bands of PBNCs[27]. The spectrum of PBNCs-DOX nanocomposites also showed characteristic DOX absorption peaks at 1571 cm^{-1} (attributed to the C=C stretching vibration in aromatic ring) and 1108 cm^{-1} (attributed to the C-O stretching vibration in the C-OH), which confirmed the successful loading of DOX into PBNCs.

The successful loading of DOX into PBNCs could be also confirmed by UV-VIS-NIR absorption and fluorescence emission spectra. As shown in Fig. 3C, the PBNCs-DOX nanocomposites displayed the characteristic absorption peak of DOX at 490 nm, and the broad absorption band of the PBNCs from 600 nm to 900 nm, which was attributed to the charge transfer transition between Fe^{2+} and Fe^{3+} in PBNCs[30]. The strong NIR region (700-900 nm) absorption was essential for NIR light driven photothermal application. In addition, compared to the strong fluorescence emission of free DOX, the fluorescence signal from DOX in PBNCs-DOX was almost completely quenched (Fig. 3D), which could occur when the fluorophores attached to a metal nanoparticle surface with close proximity[12].

3.2 DOX loading efficiency and pH/photothermal-responsive drug release

The amount of DOX loaded into PBNCs was evaluated by measuring the fluorescence intensities of the loaded DOX in our nanocomposites, and calculated from the standard curve. According to the methods described in the Experimental section, the encapsulation efficiency (88.4%) and the loading content (33.0%) were calculated. The high drug loading capability should be attributed to the big interior cube-shaped cavity of PBNCs, simple π–π stacking and hydrophobic interactions. These results suggested the great potential of PBNCs as drug delivery vehicles.

The DOX released from PBNCs-DOX nanocomposites was measured under different buffer conditions at pH7.4, 6.5 and 4.8, which was used to simulate the corresponding physiological environments of normal physiological environment, tumor cell environment and acidic cellular endosomes, respectively. As shown in Fig. 4A, the DOX released more rapidly from PBNCs at pH value of 4.8 than those at pH value of 7.4 or 6.5; meanwhile, the released amount of DOX was 25.5% ± 0.3% at pH value of 4.8 compared with 10.6% ± 0.3% and 9.8% ± 0.2% at pH value of 6.5 and 7.4 after 15 h release, respectively. These results can be explained by the protonation of amino group in DOX molecule and the increased solubility at low pH value[31].

Whether the DOX release from PBNCs-DOX could be triggered by the NIR laser was also investigated. During the DOX release experiments in buffer conditions of pH 4.8, 6.5 and 7.4, the solutions were irradiated for 5 min at each incubation time

point of 1, 2, 3, 4, 5, 6, 7, 9, 11, 13, 15 h. As shown in Fig. 4A, after the irradiation at 1 h, the cumulative release of DOX rapidly increased from 3.1 ± 0.1% to 9.5 ± 0.06% at pH 4.8, from 1.0 ± 0.03% to 3.0 ± 0.03% at pH 6.5 and from 0.9 ± 0.01% to 2.8 ± 0.04% at pH 7.4, respectively. The enhanced DOX release under NIR laser irradiation could be attributed to heat generated from the photothermal effect of PBNCs-DOX nanocomposites, which could accelerate the DOX dissolution from PBNCs. These results demonstrate that the DOX release behaviour from PBNCs-DOX nanocomposites could be triggered by pH and NIR laser irradiation.

3.3 In vitro cytotoxicity

One of the most concerns of nanoparticle for biomedical application is the toxicity[32]. Therefore, the cytotoxicity of PBNCs and PBNCs-DOX nanocomposites was evaluated by CCK-8 assay of the cell viabilities on noncancerous NIH/3T3 cells. As shown in Fig. 5A, the cell viabilities of NIH/3T3 cells maintained above 85% even under the high incubation concentration of 100 μg/mL after incubating with PBNCs for 24 h. These results suggested the good biocompatibility and no obvious cytotoxicity of PBNCs for noncancerous NIH/3T3 cells. However, after loaded with DOX, the PBNCs-DOX nanocomposites exhibited significant cytotoxicity on the cells and the cell viability decreased to 48.3 ± 11.1% at the DOX concentration of 50 μg/mL, this was ascribed to the high cytotoxicity of the released DOX on NIH/3T3 cells[33].

3.4 Temperature elevation induced by NIR laser irradiation

The evaluation of photothermal performance of PBNCs was carried out by monitoring the temperature of 1.0 mL PBNCs aqueous solution at gradient concentrations (0, 12.5, 25, 50, 100 μg/mL) induced by 808 nm laser irradiation **(**2 W/cm^2**)**. As shown in Fig. 4B, the temperature of PBNCs aqueous solution at concentration of 12.5 μg/mL was rapidly raised from 27.7 ℃ to 48.4 ℃ after 300 s NIR laser irradiation. While the concentration of PBNCs aqueous solution increased upto 100μg/mL, the temperature even reached to 83.9℃, which is sufficient to kill cancer cells[34]. As control, the temperature of pure water (0 μg/mL) was only increased from 27.4 ℃ to 34.8 ℃. These results clearly demonstrated that PBNCs exhibited a better photothermal effect than those photothermal agents based on Prussian Blue nanoparticles[5, 21, 30], and could convert the 808 nm laser energy into heat very efficiently. In addition, the similar photothermal performance of PBNCs-DOX nanocomposites was observed at the same concentration (Fig. 4C), which indicates that the photothermal effect of PBNCs could almost not be affected after the loading of DOX.

3.5 Cancer cell ablation efficiency of PBNCs-DOX nanocomposites

As discussed above, the PBNCs-DOX nanocomposites display excellent phototherapy and highly chemotherapy drug loading ability, so the combinated therapeutic effect to cancer cells was further investigated. The combinated therapeutic

effect of as-synthesis composites were qualitatively evaluated by confocal imaging of HepG2 liver cancer cells with or without NIR laser irradiation. After incubated with PBNCs-DOX nanocomposites (DOX concentration: 25 μg/mL) or PBNCs with corresponding concentration for 24 h, HepG2 cells were irradiated with NIR laser (808 nm, 2W/cm^2) for 2 min. Then the cells were stained by fluorescence dye calcein AM, which could selectively permeate into living cell. As shown in Fig. 6, green fluorescence of calcein AM was hardly seen in the cells incubated with PBNCs-DOX nanocomposites and irradiated under NIR laser, which indicated that HepG2 cells were nearly completely killed under the combination of photothermal therapy and chemotherapy. However, only a part of HepG2 cells were killed under either incubation with PBNCs-DOX nanocomposites alone or irradiation with NIR laser alone in the presence of PBNCs. Meanwhile no apparent cell death was observed under incubation with PBNCs alone, which means the neglected cytotoxicity of PBNCs.

We further quantitatively evaluated the combinated therapeutic effect of our nanocomposites on HepG2 cells using CCK-8 assay after incubation with different concentration of PBNCs and PBNCs-DOX nanocomposites. As shown in Fig. 5B, the cell viability of HepG2 cells incubated with PBNCs alone was above 85% at any observed concentration. Moderate cell viabilities were obtained when treated with PBNCs-DOX nanocomposites in the absence of NIR irradiation (63.7 ± 7.4%), free DOX in the absence of NIR irradiation (57.3 ± 3.2%), or PBNCs in the presence of

NIR irradiation (39.3 ± 6.2 %) at the observed maximum concentration. However, less than 14.6 ± 1.1% of the PBNCs-DOX nanocomposites treated cells were still alive with NIR irradiation. These results suggested that the PBNCs-DOX nanocomposites could combine the photothermal therapy and chemotherapy under NIR laser irradiation, and exhibited better therapeutic effect than any single therapeutic strategy alone.

3.5 Confocal microscopy study of cellular uptake of PBNCs-DOX

To investigate the cellular uptake and localization of the PBNCs-DOX nanocomposites in HepG2 cells, confocal microscopy fluorescence imaging was performed. HepG2 cells were incubated with PBNCs-DOX nanocomposites (10 μg/mL), whereas the HepG2 cells only incubated with culture medium were used as a control. As shown in Fig. 7, the red fluorescence of the released DOX from PBNCs-DOX nanocomposites in treated cells clearly showed the effective internalization of nanocomposites, which was not observed in control group. To further determine the subcellular localization of nanocomposites, the bright filed images were added to overlay with the red DOX fluorescence and the blue fluorescence of nuclear that is stained with DAPI. Based on these merged images, we can confirm that most of the nanocomposites were localized in the peri-nuclear regions, which clearly demonstrated the internalization of the PBNCs-DOX nanocomposites.

To investigate more details of the cellular uptake of the nanoparticles and the pH sensitive drug release behaviour inside the cells, we used Hoechst 33342 and LysoTracker Green DND-26 to stain the cell nuclei and lysosome, respectively. As shown in Fig. 8, the PBNCs-DOX nanocomposites displayed a clear co-localization with LysoTracker green after 1 h incubation, indicating the nanocomposites taken up by HepG2 cells was delivered to lysosomes and then DOX was released from the nanocages in the lysosomes. With the increasing of incubation time, more red fluorescence of DOX can be observed in the cells; after 24 h incubation, the red fluorescence signals of DOX can be clearly found in the nuclei. These results suggested that the internalized nanocomposites were delivered to lysosomes where the acidic enviroment accelerated the release and then promoted the nuclei entrance of DOX 35. In contrast, free DOX was found to localize in the nuclei only with 1 h incubation, since free DOX (a small molecule) can be quickly transported into cells and enter the active site (nuclei) by passive diffusion[36].

Furthermore, the NIR laser-triggered drug release behaviour of PBNCs-DOX nanocomposites could be also observed in the cells (Fig. 9). Compared with the cells incubated with the nanocomposites without NIR laser irradiation, a higher red fluorescence intensity of the released DOX could be seen in the cytoplasm of the cells under the NIR laser irradiation, and some of DOX fluorescence even appeared in the cell nuclei. In contrast, there were no increasing of the DOX fluorescence signals in the free DOX-treated cells under the NIR laser irradiation comapring to those without

irradiation. However, the fluorescence in these free DOX-treated cells was much higher than those in the nanocomposites-treated cells; meanwhile, most of the fluoresence signals accumulated in the nuclei in the free-DOX treated cells, due to the rapid membrane transport of small chemical molecules by passive diffusion.

4 Conclusions

In summary, the PBNCs-DOX nanocomposites were successfully developed for combining photothermal therapy with chemotherapy for the ablation of hepatocellular carcinoma cells. The PBNCs showed excellent biocompatibility, high photothermal conversion efficiency, and relatively high drug loading efficiency for DOX. The PBNCs-DOX nanocomposites under NIR laser irradiation showed significant enhancement of therapeutic effect on hepatocellular carcinoma cells (HepG2 cells) than any individual therapy approach alone in vitro. Therefore, PBNCs-DOX nanocomposites, which have integrated the photothermal therapy together with chemotherapy, could serve as promising dual-mode therapeutic agents for HCC treatment in the future.

5 Acknowledgements

This work is supported by the key clinical specialty discipline construction program of Fujian, P. R.C., the key project of National Science and technology of China (Grant No. 2012ZX10002010-001-006, and Grant No. 2012ZX10002016-013), the National Natural Science Foundation of China (Grant No. 31201008), the Key

Project of Fujian Province (Grant No. 2013YZ0002-3), the Scientific Foundation of Fuzhou Health Department (Grant No.2013-S-wq12, and Grant No.2014-S-w22), the scientific innovation project of Fujian provincial Health and Family Planning Commission (Grant No. 2014-CX-32).

Notes and references

[a] The United Innovation of Mengchao Hepatobiliary Technology Key Laboratory of Fujian Province, Mengchao Hepatobiliary Hospital of Fujian Medical University, Fuzhou 350025, P. R. China

[b] The Liver Center of Fujian Province, Fujian Medical University, Fuzhou 350025, P. R. China

[c] Liver Disease Center, The First Affiliated Hospital of Fujian Medical University, Fuzhou 350005, P. R. China

* Corresponding Author (correspondence should be address to Xiaolong Liu and Jingfeng Liu) E-mail addresses: xiaoloong.liu@gmail.com, drjingfeng@126.com

# These authors contributed equally to this work

List of abbreviation

PTCA: photothermal conversion agent; PTT: photothermal therapy; PBNCs: Prussian Blue nanocages; DOX: doxorubicin; FI: Fluorescence Intensity; NIR: Near infra-red; PBNCs-DOX: Prussian Blue nanocages loaded with doxorubicin; HCC:

hepatocellular carcinoma; CCK-8: Cell Counting Kit-8; PDI: polydispersity index; DAPI: 4',6-diamidino-2-phenylindole.

References

1 M. Ho and H. Kim, *Eur. J. Cancer*, 2011, **47**, 333-338.

2 X. Wang, A. Zhang and H. Sun, *Hepatology*, 2013, **57**, 2072-2077.

3 M. Fujimori, H. Takaki, A. Nakatsuka, J. Uraki, T. Yamanaka, T. Hasegawa, K. Shiraki, Y. Takei, H. Sakuma and K. Yamakado, *J. Vasc. Interv. Radiol.*, 2013, **24**, 655-666.

4 P. Huang, P. Rong, J. Lin, W. Li, X. Yan, M. G. Zhang, L. Nie, G. Niu, J. Lu, W. Wang and X. Chen, *J. Am. Chem. Soc.*, 2014, **136**, 8307-8313.

5 G. Fu, W. Liu, S. Feng and X. Yue, *Chem. Commun.*, 2012, **48**, 11567-11569.

6 Z. Zha, X. Yue, Q. Ren and Z. Dai, *Adv. Mater.*, 2013, **25**, 777-782.

7 J. You, P. Zhang, F. Hu, Y. Du, H. Yuan, J. Zhu, Z. Wang, J. Zhou and C. Li, *Pharm. Res.*, 2014, **31**, 554-565.

8 Z. Zhang, J. Wang and C. Chen, *Adv. Mater.*, 2013, **25**, 3869-3880.

9 X. Liu, Q. Wang, C. Li, R. Zou, B. Li, G. Song, K. Xu, Y. Zheng and J. Hu, *Nanoscale*, 2014, **6**, 4361-4370.

10 S. M. Lee, H. J. Kim, S. Y. Kim, M. K. Kwon, S. Kim, A. Cho, M. Yun, J. S. Shin and K. H. Yoo, *Biomaterials*, 2014, **35**, 2272-2282.

11 H. Jang, Y. K. Kim, H. Huh and D. H. Min, *ACS Nano*, 2014, **8**, 467-475.

12 J. You, G. Zhang and C. Li, *ACS Nano*, 2010, **4**, 1033-1041.

13 S. P. Sherlock, S. M. Tabakman, L. Xie and H. Dai, *ACS Nano*, 2011, **5**, 1505-1512.

14 K. Dong, Z. Liu, Z. Li, J. Ren and X. Qu, *Adv. Mater.*, 2013, **25**, 4452-4458.

15 H. J. Lee, Y. Liu, J. Zhao, M. Zhou, R. R. Bouchard, T. Mitcham, M. Wallace, R. J. Stafford, C. Li, S. Gupta and M. P. Melancon, *J. Control. Release*, 2013, **172**, 152-158.

16 J. You, R. Zhang, G. Zhang, M. Zhong, Y. Liu, C. S. Van Pelt, D. Liang, W. Wei, A. K. Sood and C. Li, *J. Control. Release*, 2012, **158**, 319-328.

17 R. Gui, A. Wan, X. Liu and H. Jin, *Chem. Commun.*, 2014, **50**, 1546-1548.

18 S. M. Lee, H. Park and K. H. Yoo, *Adv. Mater.*, 2010, **22**, 4049-4053.

19 http://www.fda.gov/drugs/emergencypreparedness/bioterrorismanddrugpreparedness/ucm130334.htm.

20 L. Jing, X. Liang, Z. Deng, S. Feng, X. Li, M. Huang, C. Li and Z. Dai, *Biomaterials*, 2014, **35**, 5814-5821.

21 H. A. Hoffman, L. Chakrabarti, M. F. Dumont, A. D. Sandler and R. Fernandes, *RSC Adv.*, 2014, **4**, 29729-29734.

22 G. Fu, W. Liu, Y. Li, Y. Jin, L. Jiang, X. Liang, S. Feng and Z. Dai,

Bioconjugate Chem., 2014, **25**, 1655-1663.
23 L. Cheng, H. Gong, W. Zhu, J. Liu, X. Wang, G. Liu and Z. Liu, *Biomaterials*, 2014, **35**, 9844-9852.
24 M. Hu, S. Furukawa, R. Ohtani, H. Sukegawa, Y. Nemoto, J. Reboul, S. Kitagawa and Y. Yamauchi, *Angew. Chem.*, 2012, **124**, 1008-1012.
25 H. Lian, M. Hu, C. Liu, Y. Yamauchi and K. C. W. Wu, *Chem. Commun.*, 2012, **48**, 5151-5153.
26 Q. Zhang, T. Zhang, J. Ge and Y. Yin, *Nano Lett.*, 2008, **8**, 2867-2871.
27 T. Uemura and S. Kitagawa, *J. Am. Chem. Soc.*, 2003, **125**, 7814-7815.
28 M. Wu, X. M. Xia, C. Cui, P. Yu, Y. Zhang, L. Liu, R. X. Zhuo and S. W. Huang, *J. Mater. Chem. B*, 2013, **1**, 1687-1695.
29 R. Hachani, M. Lowdell, M. Birchall and N. n. T. K. Thanh, *Nanoscale*, 2013, **5**, 11362-11373.
30 Z. Li, Y. Zeng, D. Zhang, M. Wu, L. Wu, A. Huang, H. Yang, X. Liu and J. Liu, *J. Mater. Chem. B*, 2014, **2**, 3686-3696.
31 H. Gong, L. Cheng, J. Xiang, H. Xu, L. Feng, X. Shi and Z. Liu, *Adv. Funct. Mater.*, 2013, **23**, 6059-6067.
32 Y. Liu, K. Ai, J. Liu, Q. Yuan, Y. He and L. Lu, *Angew. Chem. Int. Ed.*, 2012, **51**, 1437-1442.
33 M. Prabaharan, J. J. Grailer, S. Pilla, D. A. Steeber and S Gong, *Biomaterials*, 2009, **30**, 6065-6075.
34 D. Jaque, L. Martinez Maestro, B. del Rosal, P. Haro-Gonzalez and A. Benayas, J. L. Plaza, E. Martin Rodriguez and J. Garcia Sole, *Nanoscale*, 2014, **6**, 9494-9530.
35 S. Zhu, M. Hong, G. Tang, L. Qian, J. Lin, Y. Jiang and Y. Pei, *Biomaterials*, 2010, **31**, 1360-1371.
36 C. Cui, Y. Xue, M. Wu, Y. Zhang, P. Yu, L. Liu, R. Zhuo and S. Huang, *Biomaterials*, 2013, **34**, 3858-3869.

Figure caption

Fig. 1 Schematic view of the synthesis procedure of PBNCs-DOX nanocomposites.

Fig.2 TEM images of PBNCs (A), PBNCs-DOX nanocomposites obtained with initial DOX concentration of 0.25 mg/mL(B), 0.5 mg/mL (C) and free DOX obtained from a feeding concentration of 0.5 mg/mL in the absence of PBNCs(D).

Fig.3 (A) Size distribution of PBNCs and PBNCs-DOX nanocomposites measured by DLS. (B) FT-IR spectra of PBNCs (a), DOX (b) and PBNCs-DOX nanocomposites (c). (C) UV-Vis-NIR absorption spectra of PBNCs, DOX and PBNCs-DOX nanocomposites in water. (D) Fluorescence intensity of PBNCs, DOX and PBNCs-DOX nanocomposites in water.

Fig. 4 (A) The cumulative DOX release kinetics from PBNCs-DOX nanocomposites in phosphate-buffer saline (pH 7.4), phosphate-buffer saline (pH 6.5) and acetate buffer (pH 4.8) at 37 ℃. (B) Temperature change of the aqueous solution containing different concentration of PBNCs under 808 nm laser irradiation at a power density (2 W/cm^2) for 5 min. (C) Temperature change of the aqueous solution containing different concentration of PBNCs-DOX nanocomposites (with equivalent PBNCs

concentration) under 808 nm laser irradiation at a power density (2 W/cm^2) for 5 min.

Fig.5 (A) Cell viabilities of NIH/3T3 cells incubated with different concentrations of PBNCs and PBNCs-DOX nanocomposites for 24 h. (B) The cell viability of HepG2 cells incubated with DOX, PBNCs or PBNCs-DOX nanocomposites with the equivalent DOX. The cells were either irradiated with NIR laser (808nm, 2W/cm^2) for 2 min, or without laser irradiation as indicated.

Fig. 6 Photo-thermal ablation of HepG2 cells. (A) Without PBNCs and laser irradiation; (B) with PBNCs but without laser irradiation; (C) with PBNCs-DOX nanocomposites but without laser irradiation; (D) with PBNCs and laser irradiation; (E) with PBNCs-DOX nanocomposites and laser irradiation. Scale bar: 50 μm.

Fig. 7 Confocal images of HepG2 cells incubated with PBNCs-DOX nanocomposites (DOX: 10 μg/mL) in DMEM medium. Nuclei were counter-stained with DAPI. Scale bar: 20 μm.

Fig. 8 Confocal images of HepG2 cells incubated with PBNCs-DOX nanocomposites

or free DOX (10 μg/mL) for 1 h, 4 h and 24 h. Nuclei and lysosome were counter-stained with Hoechst 33342 and Lysotracker Green DND-26, respectively. Scale bar: 10 μm.

Fig. 9 Confocal images of HepG2 cells incubated with PBNCs-DOX nanocomposites or free DOX (DOX: 3μg/mL) for 4 h, then with or without NIR laser irradiation for 5 min. Nuclei were counter-stained with DAPI. Scale bar: 20 μm.

Fig. 1

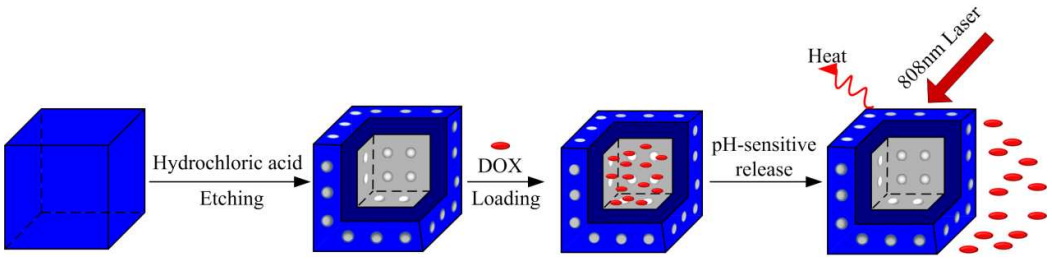

Fig. 2

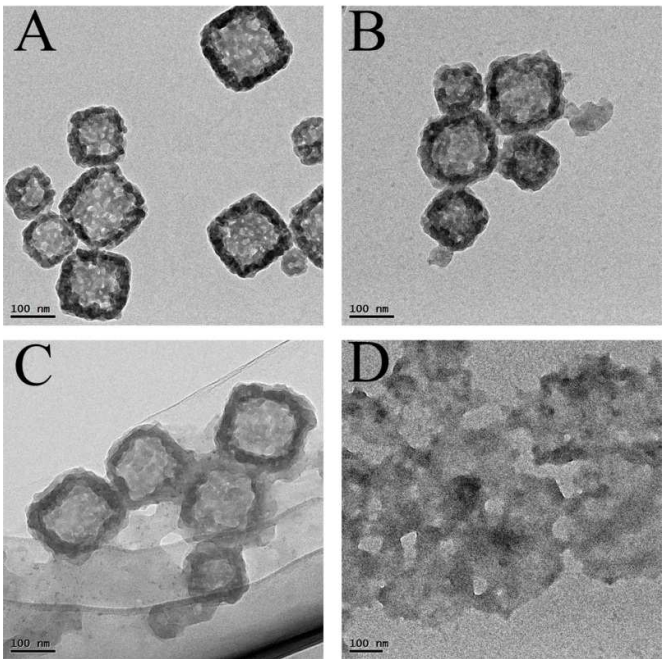

Fig. 3

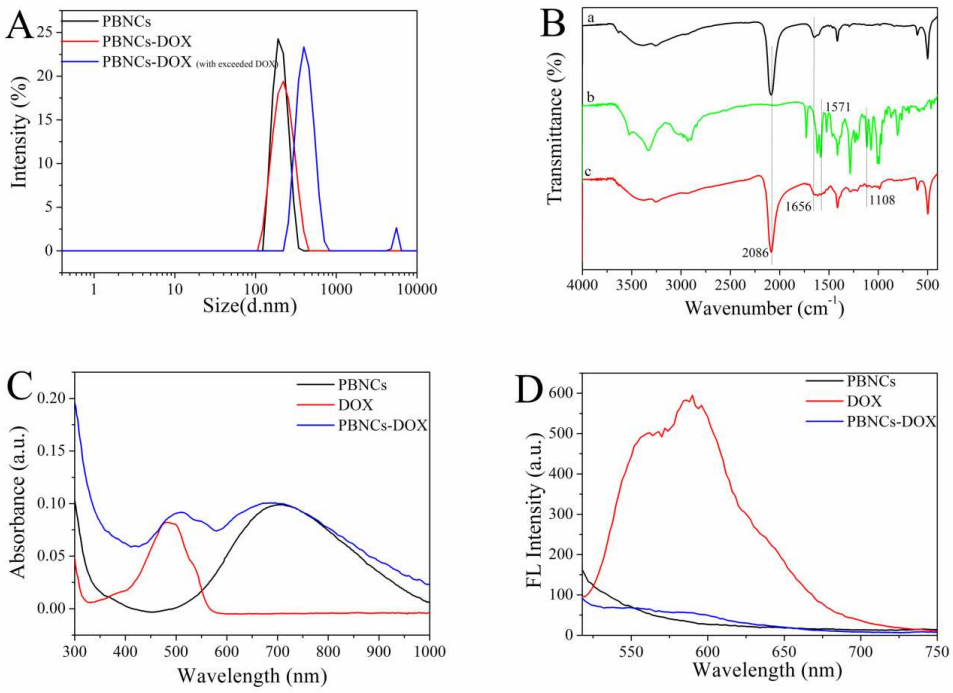

Fig. 4

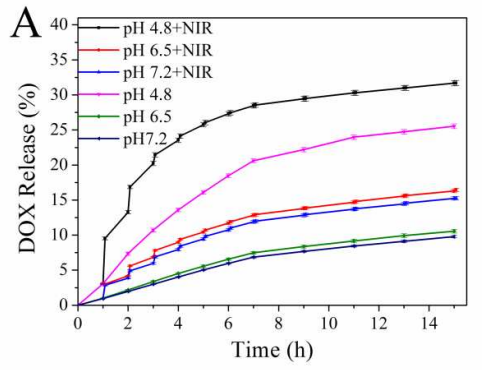

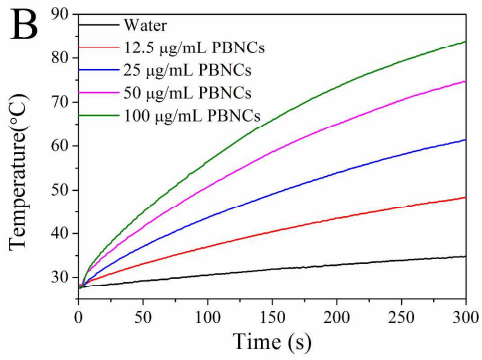

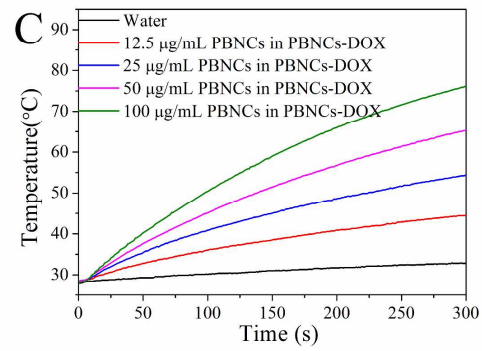

Fig. 5

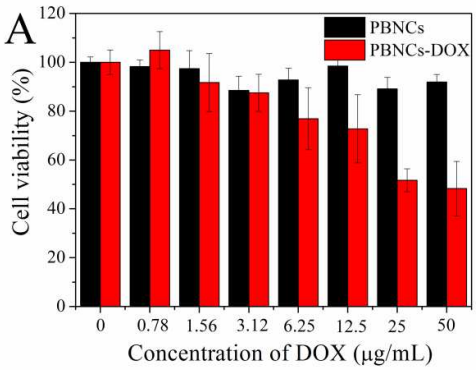

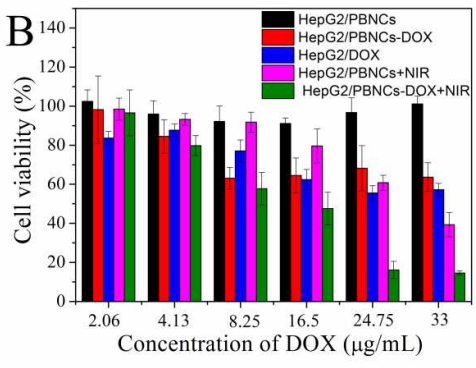

Fig. 6

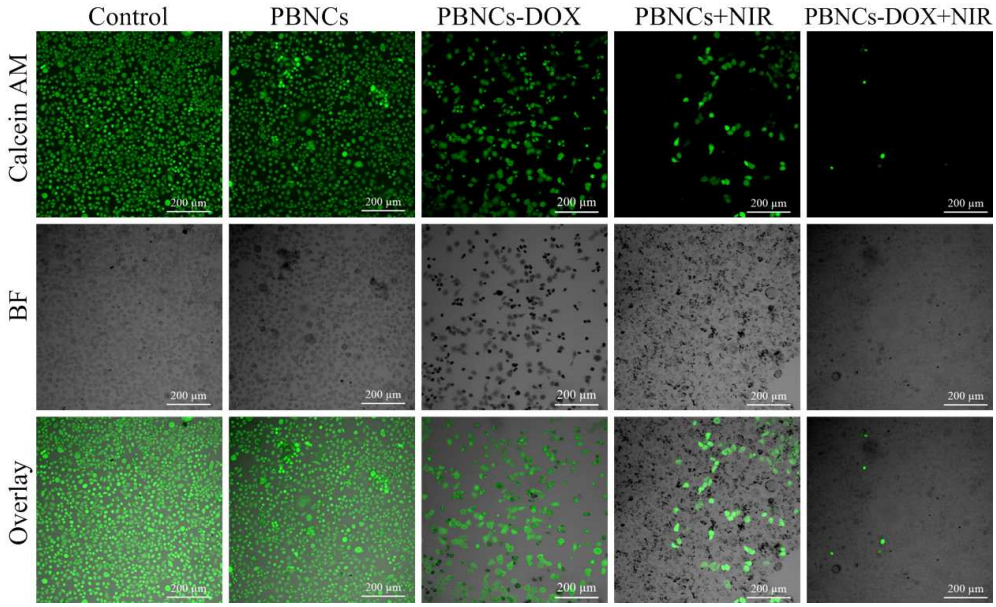

Fig. 7

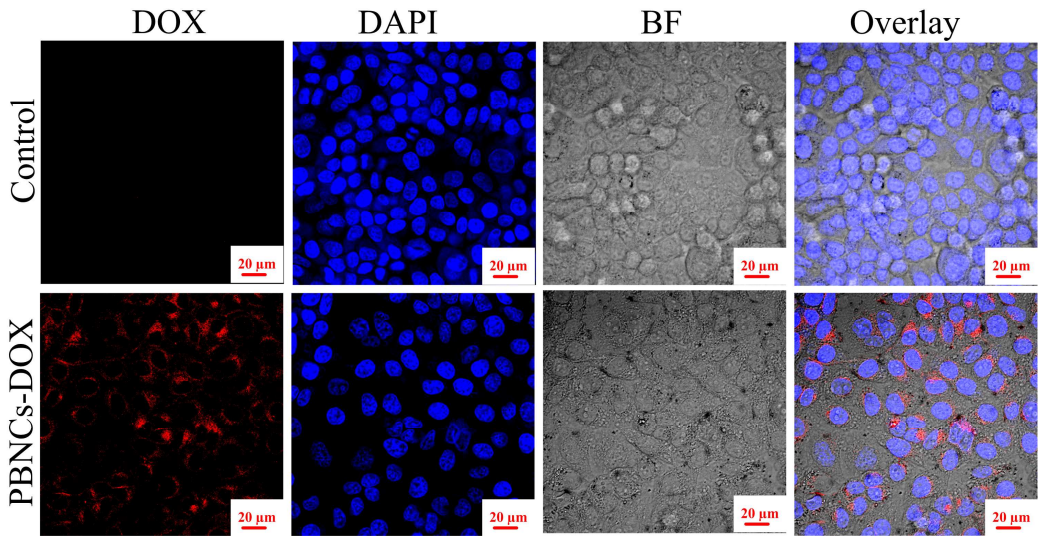

Fig. 8

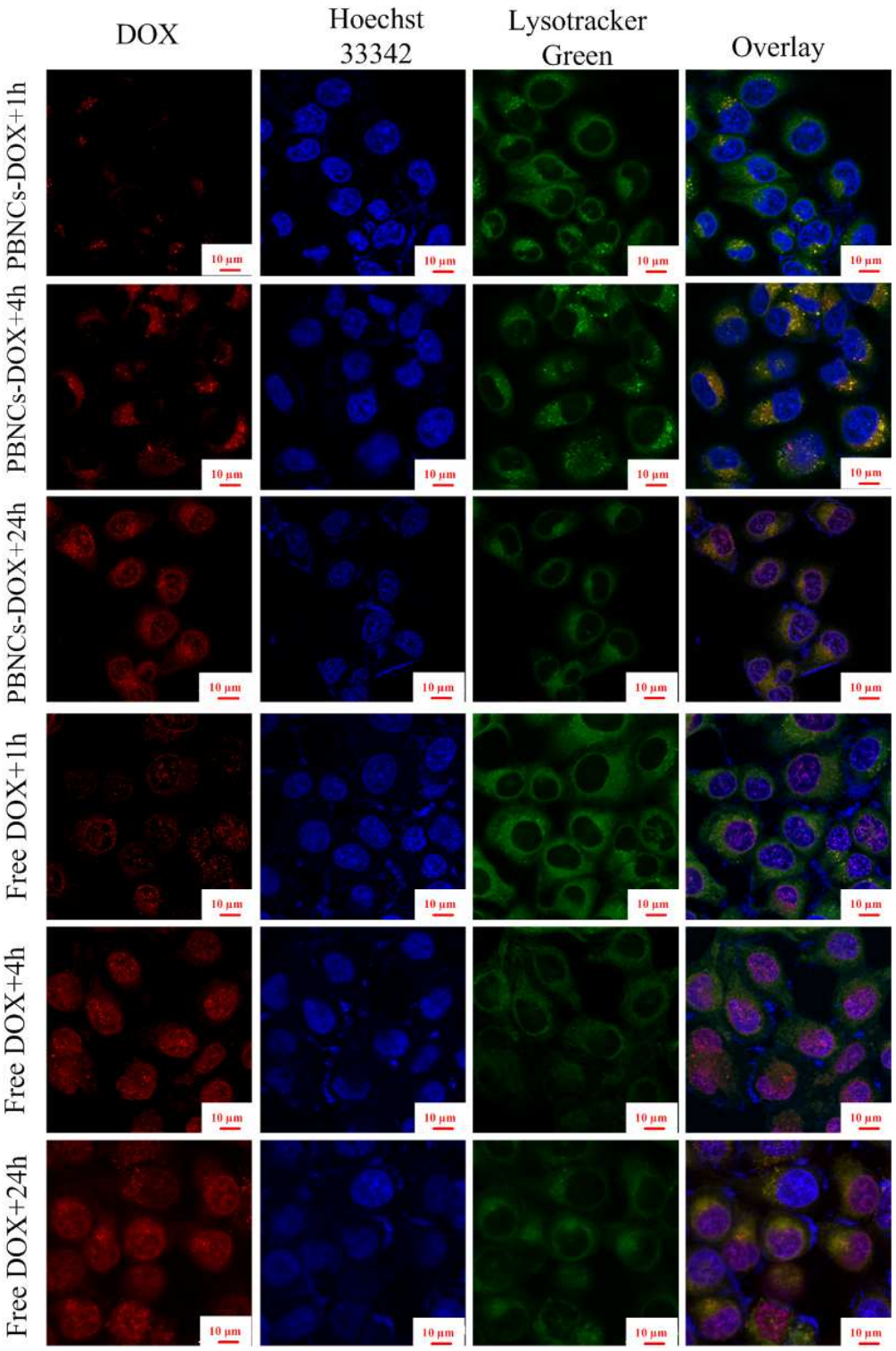

Fig. 9